



Assessment of hydrothermal parameters on alkaline activation of fly ashes using a central composite design

Iván SUPELANO GARCÍA^{1,*}, César Armando ORTÍZ OTÁLORA², Carlos Arturo PARRA VARGAS¹, and Julieth Alexandra MEJÍA GÓMEZ³

¹ Pedagogical and Technological University of Colombia, GFM Group, North central avenue 39-115 Tunja, Boyacá 150001, Colombia

² Pedagogical and Technological University of Colombia, GSEC Group, North central avenue 39-115 Tunja, Boyacá 150001, Colombia

³ Antonio Nariño University, Faculty of science, GIFAM group, avenue 7 # 21-84, Tunja, Boyacá 150002, Colombia

*Corresponding author e-mail: ivan.supelano@uptc.edu.co

Received date:

18 January 2021

Revised date:

22 May 2021

Accepted date:

24 May 2021

Keywords:

Coal fly ash;
Zeolitic materials;
Hydrothermal method;
Central composite design

Abstract

Coal fly ash (CFA) is a powder generated during combustion of coal; its improper disposal constitutes an environmental issue. To minimize this problem, one of the uses of CFA is as feedstock for production of zeolite. Different studies have shown that zeolites may be easily obtained from CFA by relatively cheap and fast conversion processes. Most of these studies have been focused on the study of the zeolite synthesis using classical methods through changing one factor per time and fixing the other factors, where it illustrates the impact of each variable individually via a huge number of experiments, however it doesn't consider the effect of the interaction between different factors under study.

This study aims to evaluate the effects of hydrothermal synthesis parameters, time of activation (t), temperature of synthesis (T) and concentration of alkaline activator ([NaOH]), on the formation of zeolite. Morphological and structural properties were determined through scanning electron microscopy and X-ray diffraction. The experiments were designed through a central composite design. The results revealed that 4M NaOH, 90°C and time synthesis of 36 h were the conditions for a higher conversion of CFA into sodalite, furthermore, it was obtained P1-Na and losod as zeolite phases.

1. Introduction

Coal fly ash (CFA) is a fine powder with primarily chemical composition of oxides of silicon, aluminum and iron [1], it is produced by coal burning in electric generation power plants and is considered a pollutant. To reduce the exposure to the environment, CFA has been used as additive in concrete production [2], aggregate in asphalt material [3], precursor in geopolymer synthesis [4] and raw material for zeolite synthesis [5], in which the hydrothermal method is the most popular route for zeolite synthesis from CFA. That consists of the alkali activation of CFA in an aqueous solution. The alkaline solution dissolves both the amorphous and crystalline silica and aluminum, increasing the concentration of Al^{3+} and Si^{4+} , condensation reactions are followed, resulting in the formation of crystal nuclei and the crystallization of zeolite phase. Finally, the product is filtered washed and dried [6]. The hydrothermal route was developed by Barrer *et al.* 1948, the method is classified into subcritical if the temperature of synthesis is between 100°C to 240°C or supercritical when the temperature reaches up to 1000°C [7], simple hydrothermal synthesis is known as one-step synthesis and has been used by several authors [1,9-15] where alkaline activator, the concentration of alkaline activator, the temperature of synthesis, the time of synthesis, the Si/Al ratio and the solid/liquid ratio are the main factors that influence the synthesis route [8]. Furthermore, fusion step previous to hydrothermal

treatment in which the CFA is mixed with solid Na precursor and heated at temperatures until 850°C has been reported [16-23], or modification of hydrothermal method i.e. microwave heating has been reported [24-25].

Table 1 summarizes experimental conditions of zeolite synthesized by the one step hydrothermal method using CFA, it shows that activation time lies between 2 h and 96 h, temperature synthesis between 75°C and 200°C and the concentration of alkaline activator between 0.5 M and 12 M, producing 9 kinds of zeolites [1,9-15,27]. Usually, these parameters are studied by a design of experiments in which the influence of one variable at a time is studied (OVAT approach) to evaluate the best synthesis in relation with one response variable of interest, that is to say: the study of the linear effect of the factor with the response variable. In those class of experiments, it is not possible to establish the interactive effects between all variables of the study. Thus, the models of second order have been introduced to study the interactive effects, i.e. the response surface methodology is a multivariable technique developed to study the interactive effects between the studied variables [26].

In this work, we used a CCD to design a set of experiments to monitoring the formation of zeolite phase by the activation of the CFA with NaOH, at temperature of synthesis between 60°C and 95°C, concentration of alkaline activator between 1.37 M and 4.63 M and activation time between 4.5 h and 43.5 h. The central point of

Table 1. Data of synthesis conditions of one step hydrothermal method and corresponding synthesized zeolite obtained from literature.

Reference	Activation time (h)	Temperature synthesis (°C)	Alkaline activator concentration (M)	Zeolite
[1]	96	90	2	Na-P1
	67	90	2	Na-A
[9]	24	90	1	Na-P1
				Hydroxy-cancrinite
				Hydroxy-sodalite
[10]	12	150	1	Na-P1
	12	200	1	Analcime-C+Sodalite
[11]	24	75	3	Na-X
	24	105	1	Na-P1
	24	105	5	Sodalite
[12]	12	95	3	X
	12	140	3	P
	12	180	3	Analcime+Cancrinite
	4	140	1.5	X
	6	140	1.5	P
	8	140	1.5	Hydrosodalite+analcime
	6	140	3	P+Analcime
	8	140	3	P+Analcime
	6	140	4.5	P+Analcime
	8	140	4.5	P+Analcime
[13]	24	75	3	Na-X
	24	95	3	Na-P1
[14]	6	140-320	1.16	Na-P1
	6	320	1.16	Analcime
[15]	24	100-150	0.5-3.5	Na-P1
				Analcime
				Cancrinite
				Sodalite
				X
[27]	2	80	6-12	Na-P1
				Analcime

the experiment was chosen in a way that all the parameters lie between low synthesis conditions. The relative intensity between main reflection of quartz and zeolite (I_z/I_q) in the XRD pattern was selected as response variable, this ratio assesses the relative crystalline degree of the zeolite and the grade of the conversion of CFA into zeolite.

2. Experimental

2.1 Materials

Coal fly ash (CFA) was collected from silo of Sochagota Termo Paipa IV power station, Boyacá Colombia, the CFA with grain size smaller than 44 μm , obtained by sieving process, was employed as source for zeolite synthesis. Chemical analysis by using a MagixPro PW-2440 Philips (WDXRF) spectrometer reveals that the main chemical composition of CFA is SiO_2 (61.64%), Al_2O_3 (23.72%), Fe_2O_3 (7.13%), K_2O (1.55%), TiO_2 (1.45%) and CaO (1.33%).

2.2 Synthesis and analysis

Hydrothermal treatment of CFA with NaOH solution was performed as follows. CFA was added to sodium hydroxide solution in deionized

water in a Teflon vessel of 105 mL of volume, the vessel was placed within steel reactor under magnetic stirring at 500 rpm. The reactor was heated and the system was located into a thermal recipient to keep a constant temperature, which was monitored with a K thermocouple. The NaOH concentration, temperature synthesis and activation time were adjusted according to central composite design.

The measurements of X-ray diffraction (XRD) were performed by using a PANalytical X'Pert's X ray diffractometer with $K_{\alpha}\text{-Co}$ radiation ($\lambda = 1.789007 \text{ \AA}$) at room temperature within a range 2θ from 10° to 80° and a step of 0.02° . Morphology of CFA and alkaline treated samples was observed by Scanning electron microscope (SEM) technique, the images were acquired using a Carl Zeiss EVO-MA10 microscope. The equipment is coupled with energy-dispersive X-ray (EDX) analyzer, Oxford Instruments.

2.3 Experimental design

The effect of concentration of NaOH, temperature synthesis and activation time in the synthesis of zeolite from CFA, were studied by using a central composite design determined by 2^n+2n+6 , where $n = 3$ is the number of variables, $2^n = 2^3 = 8$ are factor points, $2n = 2(3) = 6$ are axial points. The ratio of axial points was calculated as $\alpha = [2^n]^{1/4} = 1.682$. The relation between real and coded values are given by:

Table 2. Factors and levels used for the central composite design.

Variable	Factor	Low value (-)	High value (+)
t (h)	X ₁	12	36
T (°C)	X ₂	60	90
NaOH (M)	X ₃	2	4

Table 3. Central composite design matrix and labeled samples

Run	t (h)	T (°C)	[NaOH] (M)	Label Sample
1	24	75	3	M1
2	24	75	3	M2
3	12	60	4	M3
4	36	60	4	M4
5	12	60	2	M5
6	36	60	2	M6
7	36	90	4	M7
8	24	75	3	M8
9	12	90	2	M9
10	24	75	3	M10
11	36	90	2	M11
12	12	90	4	M12
13	24	75	1.4	M13
14	44	75	3	M14
15	24	99.5	3	M15
16	4.44	75	3	M16
17	24	75	4.6	M17
18	24	75	3	M18
19	24	75	3	M19
20	24	51	3	M20

$$X_1 = \frac{t-24}{12} \quad (1)$$

$$X_2 = \frac{T-75}{15} \quad (2)$$

$$X_3 = [\text{NaOH}] - 3 \quad (3)$$

where t is the activation time, T the temperature synthesis and [NaOH] the concentration of alkaline activator. A, B and C are the coded variables. Table 2 and Table 3 summarize the coded values with corresponding levels and the set of experiments in a random order.

The intensity ratio between the amplitude of the diffraction peak of main zeolite phase and quartz phase (I_z/I_Q) was chosen as dependent variable.

3. Results and discussion

The crystalline phases of CFA and after the hydrothermal treatment were determined. The XRD results of CFA show three crystalline phases: quartz (PDF card N° 01-083-0539), mullite (PDF card N° 01-079-1275) and iron oxide (PDF card N° 00-024-0072). In all experiments described in Table 3, the quartz phase coming from CFA was identified. Zeolitic materials were not detected in samples M5 and M20 and no transformation were observed after hydrothermal treatment, whereas a transformation with at least one zeolite structure was recognized in other experiments, samples M1 to M4 and M6 to M19. Five types of zeolite were identified in the set of experiments: three of P1-Na: PDF card N° 00-039-0219 $\text{Na}_6\text{Al}_6\text{Si}_{10}\text{O}_{32} \cdot 12\text{H}_2\text{O}$, PDF card N°

00-025-0778 $\text{Na}_3\text{Al}_3\text{Si}_5\text{O}_{16} \cdot 6\text{H}_2\text{O}$ and PDF card N° $\text{Na}_6\text{Al}_6\text{Si}_{10}\text{O}_{32}(\text{H}_2\text{O})_{12}$; sodalite PDF card N° 01-076-1639 $\text{Al}_6\text{H}_6\text{Na}_8\text{O}_{28}\text{Si}_6$; and losod PDF card N° 00-031-1269 $\text{Na}_{12}\text{Al}_{12}\text{Si}_{12}\text{O}_{48} \cdot x\text{H}_2\text{O}$. Figure 1 shows the XRD patterns taken at room temperature for all samples. The figure depicts the main reflection of those structures.

The principal reflection of quartz is due to the (011) diffraction plane, its relative height varies among the samples indicating a different grade of conversion of the amorphous CFA into new products. The intensity of the reflections due to (011) diffraction plane of quartz and the (110) (for P1-Na PDF cards N° 00-039-0219 and 00-025-0778; Sodalite and Losod) or (101) (for P1-Na PDF cards N° 00-039-0219 and 01-071-0962) in the corresponding zeolite structure, were selected to calculate the I_z/I_Q ratio. The data of first three reflections are listed in Table 4.

A general trend was observed in the results: the intensity of diffraction peaks related to crystalline phases coming from CFA decreases and the intensity of diffraction peaks related to zeolite phase increases when the time of synthesis, temperature or alkaline concentration increases. The peaks of zeolite exhibit a shift between them, it is due to the little change in the lattice parameters. Table 4 lists the first reflections of main synthesized zeolite and the I_z/I_Q ratio.

The data of I_z/I_Q ratio was fitted with a quadratic equation model to observe the effects of the independent parameters: NaOH concentration, temperature and activation time according to Equation (4):

$$Y = \beta_0 + \sum_{i=1}^k \beta_i \cdot X_i + \sum_{i=1}^k \beta_{ii} \cdot X_i^2 + \sum_{i,j}^k \beta_{ij} \cdot X_i \cdot X_j \quad (4)$$

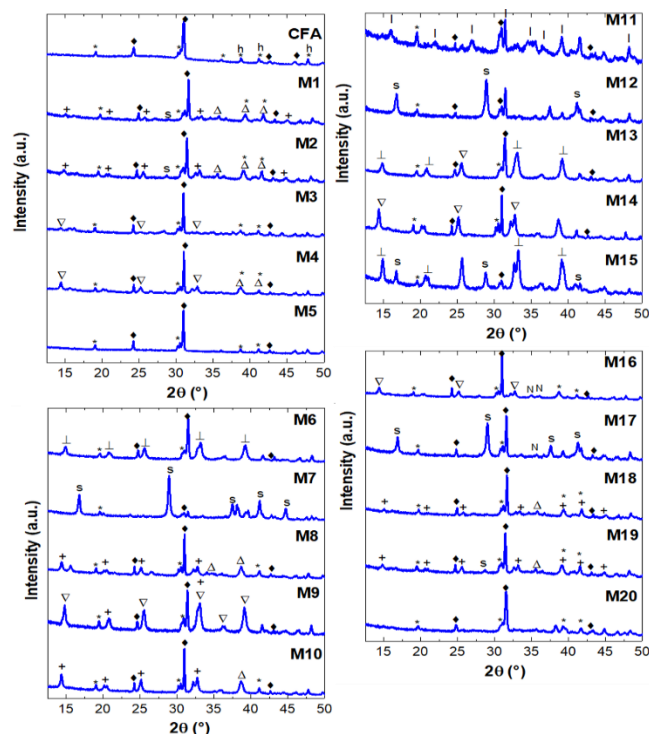


Figure 1. XRD patterns of CFA and samples M1 to M20. • quartz SiO_2 ; * mullite $\text{Al}_{4.80}\text{O}_{9.60}\text{Si}_{1.20}$; \dagger iron oxide Fe_2O_3 ; + P1-Na $\text{Na}_6\text{Al}_6\text{Si}_{10}\text{O}_{32} \cdot 12\text{H}_2\text{O}$; \wedge P1-Na $\text{Na}_3\text{Al}_3\text{Si}_5\text{O}_{16} \cdot 6\text{H}_2\text{O}$; ∇ P1-Na $\text{Na}_6\text{Al}_6\text{Si}_{10}\text{O}_{32}(\text{H}_2\text{O})_{12}$; \square sodalite $\text{Al}_6\text{H}_6\text{Na}_8\text{O}_{28}\text{Si}_6$; \diamond losod $\text{Na}_{12}\text{Al}_{12}\text{Si}_{12}\text{O}_{48} \cdot x\text{H}_2\text{O}$; $\bar{\mid}$ sodium silicate $\text{C}_2\text{Na}_8\text{O}_{10}\text{Si}$; \mid zeolite A $\text{Na}_{96}\text{Al}_{96}\text{Si}_{96}\text{O}_{384} \cdot 216\text{H}_2\text{O}$ PDF card N° 00-039-0222.

Table 4. List of main synthesized zeolite phases with its corresponding foremost reflections and the I_z/I_Q ratio.

	Zeolite	PDF card N°	2θ (°)	(hkl)	I_z/I_Q Ratio
M1	P1-Na	00-039-0219	14.35	(110)	0.49
			25.18	(211)	
			32.75	(301)	
M2	P1-Na	00-039-0219	14.58	(101)	0.44
			25.34	(211)	
			32.95	(301)	
M3	P1-Na	01-071-0962	14.81	(101)	0.26
			25.54	(121)	
			32.85	(301)	
M4	P1-Na	01-071-0962	14.42	(101)	0.33
			25.21	(121)	
			32.85	(301)	
M6	P1-Na	00-025-0778	14.91	(110)	0.41
			25.62	(211)	
			33.21	(310)	
M7	Sodalite	01-076-1639	16.78	(110)	2.27
			23.62	(200)	
			28.97	(211)	
M8	P1-Na	00-039-0219	14.46	(101)	0.43
			25.20	(211)	
			32.83	(301)	
M9	P1-Na	01-071-0962	14.79	(101)	0.71
			25.51	(121)	
			33.09	(301)	
M10	P1-Na	00-039-0219	14.38	(101)	0.49
			25.19	(211)	
			32.81	(301)	
M11	Losod	00-031-1269	16.00	(110)	0.77
			21.95	(101)	
			26.95	(201)	
M12	Sodalite	01-076-1639	16.75	(110)	0.87
			23.63	(200)	
			28.92	(211)	
M13	P1-Na	00-025-0778	14.83	(110)	0.50
			25.55	(211)	
			33.08	(310)	
M14	P1-Na	01-071-0962	14.36	(101)	0.73
			25.14	(121)	
			32.76	(301)	
M15	P1-Na	00-025-0778	14.86	(110)	1.93
			25.61	(211)	
			33.25	(310)	
M16	P1-Na	01-071-0962	14.44	(101)	0.32
			25.16	(121)	
			32.74	(301)	
M17	Sodalite	01-076-1639	16.88	(110)	0.59
			23.77	(200)	
			29.04	(211)	
M18	P1-Na	00-039-0219	15.04	(101)	0.33
			24.90	(211)	
			33.39	(301)	
M19	P1-Na	00-039-0219	14.88	(101)	0.38
			25.62	(211)	

Where β_i are the coefficients of first order, β_{ii} are the coefficients of quadratic effects, β_{ij} are the coefficients of interaction effects, k the number of factors and X_i the factors. Using the analysis of variance (ANOVA), the fitted coefficients for the polynomial equation were calculated. Equation (5) gives the I_z/I_Q ratio as a function of single, quadratic and interacting parameters in terms of coded variables.

$$\begin{aligned} I_z/I_Q = & 0.429 + 0.191X_1 + 0.513X_2 + 0.144X_3 \\ & + 0.033X_1^2 + 0.198X_2^2 + 0.041X_3^2 \\ & + 0.131X_1X_2 + 0.116X_1X_3 + 0.194X_2X_3 \end{aligned} \quad (5)$$

Table 5 summarizes the estimated effects, with agreement values $S = 0.21$, $R^2 = 93.9\%$ and $R^2_{fit} = 85.6\%$ of the model, it means that the quadratic model used to fit the data is satisfactory and it indicates good predictability. The significance of the effect was calculated at a p -value of 0.05, it denotes that effects with p -value lower than 0.05 has a high statistical significance. In relation with p -value, the $X_1 * X_1$ and $X_3 * X_3$ terms of the model are not significant, thus, without consider these terms the new Equation (5) reduces to:

$$\begin{aligned} I_z/I_Q = & 0.481 + 0.191X_1 + 0.513X_2 + 0.144X_3 \\ & + 0.193X_2^2 + 0.131X_1X_2 + 0.116X_1X_3 \\ & + 0.194X_2X_3 \end{aligned} \quad (6)$$

with new agreement values: $S = 0.19$, $R^2 = 93.4\%$ and $R^2_{fit} = 87.4\%$ that improve the model. All the coefficients obtained are positive, it indicates that CFA conversion is increased with increasing the values of the factors t , T or $[NaOH]$. The β_2 coefficient is the biggest in the model, which reveals that alkaline conversion of CFA is more sensitivity to the temperature, whereas the conversion of CFA is less sensitive to the alkaline concentration of NaOH. Figure 2 displays the I_z/I_Q dependence as a function of synthesis parameters. The plots show a higher degree of curvature when t is set to central value, and a lower degree of curvature when T is set to central value. This confirm the larger interaction between T and $[NaOH]$ variables that others one. It is evident that the CFA conversion increases as the parameters increase and there is a strong influence when the factors T and $[NaOH]$ are changed.

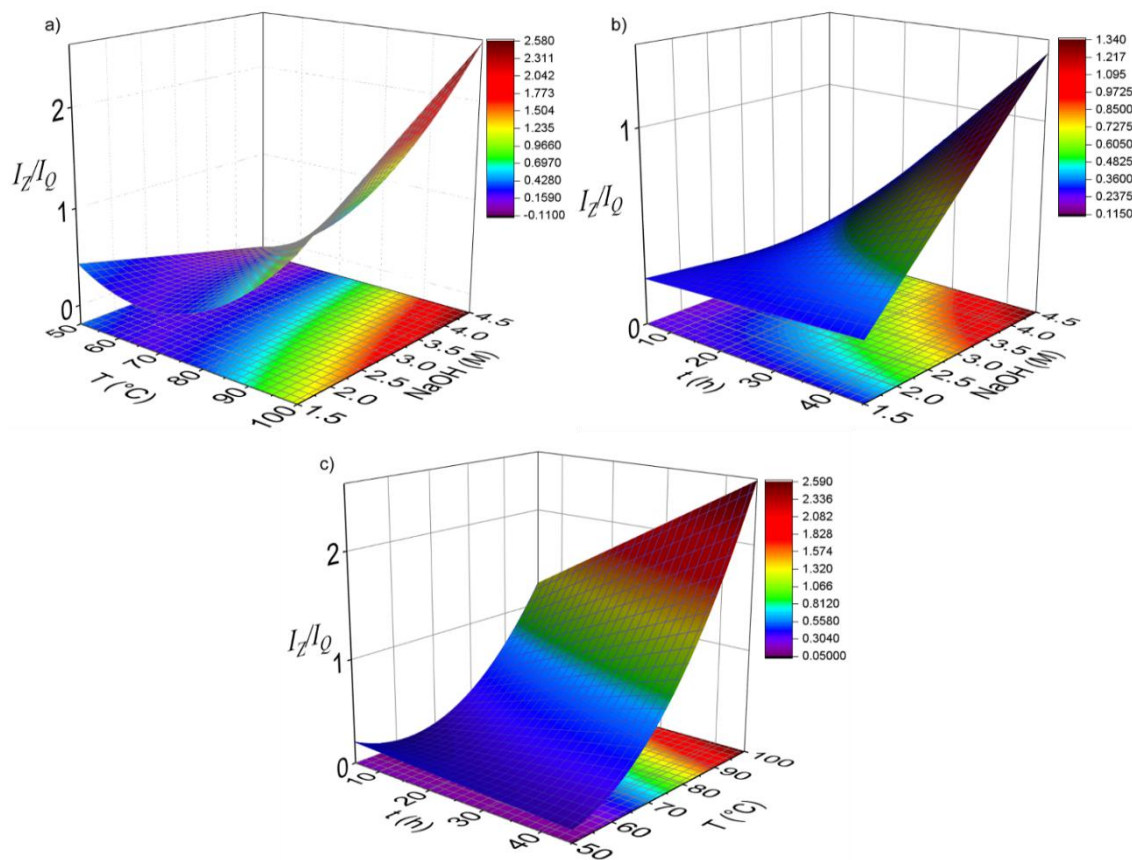
Table 5. Estimated effects of the complete quadratic model of the Equation 5.

Term	SC Ajust.	MC Ajust.	F-value	p-value
Model	5.60219	0.50929	11.30	0.001
X_1	0.48369	0.48369	10.73	0.011
X_2	3.51064	3.51064	77.89	0.000
X_3	0.27561	0.27561	6.11	0.039
$X_1 * X_1$	0.01453	0.01453	0.32	0.586
$X_2 * X_2$	0.51865	0.51865	11.51	0.009
$X_3 * X_3$	0.02185	0.02185	0.48	0.506
$X_1 * X_2$	0.13781	0.13781	3.06	0.118
$X_1 * X_3$	0.10811	0.10811	2.40	0.160
$X_2 * X_3$	0.30031	0.30031	6.66	0.033

Table 6. Estimated effects of the improved quadratic model of the Equation 6.

Term	SC Ajust.	MC Ajust.	F-value	p-value
Model	5.56818	0.61869	15.68	0.000
X_1	0.48369	0.48369	12.26	0.006
X_2	3.51064	3.51064	88.97	0.000
X_3	0.27561	0.27561	6.98	0.025
$X_2 * X_2$	0.49794	0.49794	12.62	0.005
$X_1 * X_2$	0.13781	0.13781	3.49	0.091
$X_1 * X_3$	0.10811	0.10811	2.74	0.129
$X_2 * X_3$	0.30031	0.30031	7.61	0.020

The morphological characteristics of the samples were observed by SEM technique in backscattering mode. As example, the Figure 3. shows the SEM images obtained for CFA, M18, M7, M11, M14 and M15. The CFA particles are spheroidal shape which correspond to cenospheres. The alkaline treated samples display a morphological transformation in which the spheroidal particles dissolve and particles with flake and rod shape form agglomerates. The chemical composition was checked with EDX, Figure 4, the main components detected were Fe, Si, Al and O in the CFA and Al, Si, Na, O and Fe in the alkaline treated samples.

**Figure 2.** Surface and contour map for I_z/I_0 as a function of a) temperature and concentration of NaOH b) time and concentration of NaOH and c) temperature and time.

The literature reports the synthesis of different allotypes of P1-Na from CFA under a wide variety of parameters at 96 h, 90°C, 2 M [1], 24 h, 90°C, 1 M [9], 24 h, 105°C, 1 M [11], 24 h, 95°C, 3 M [12], 6 h, 14°C to 320°C, 1.16 M [14], 24 h, 100°C to 150°C, 0.5 M to 3.5 M [15], and 2 h, 80°C, 6 M to 12 M [27]. In comparison with the literature the synthesis at 24 h, 75°C and 3 M reported by Derkowski *et al.* [11] match with the experimental conditions of the synthesis of the M1, M2, M8, M10, M18 and M19 samples in this work. Derkowski *et al.* [11] obtained a Na-X zeolite with presence of mullite and quartz, the difference between that work and our work is that we obtained P1-Na zeolite, the main difference between two experiments is the chemical composition of CFA.

The synthesis and conversion grade of a characteristic zeolite from CFA depend on the activation time, temperature synthesis and alkaline concentration, the chemical composition and other variables as the CFA/solution ratio.

In this work the larger conversion of CFA was reached for the CFA treated at 36 h, 90°C and 4 M, the statistical model describes that CFA conversion is strongly affected by temperature synthesis, it joined with the high interaction effect between T and [NaOH]. According to the Höller and Wirsching mechanism [28] (which explain the conversion of CFA into zeolite in terms of the dissolution of CFA by the NaOH followed by condensation, nucleation and growth of zeolite), together with the results of the statistical model suggest that the temperature and the interaction effect between T and [NaOH] on the synthesis of CFA into different zeolites structures influence the dissolution and crystal growth steps, thus the relative content of the quartz phase varies and changes the I_z/I_0 ratio. In the range of study here was possible to obtain materials with zeolite structure at relatively low conditions in comparison with that reported in the literature.

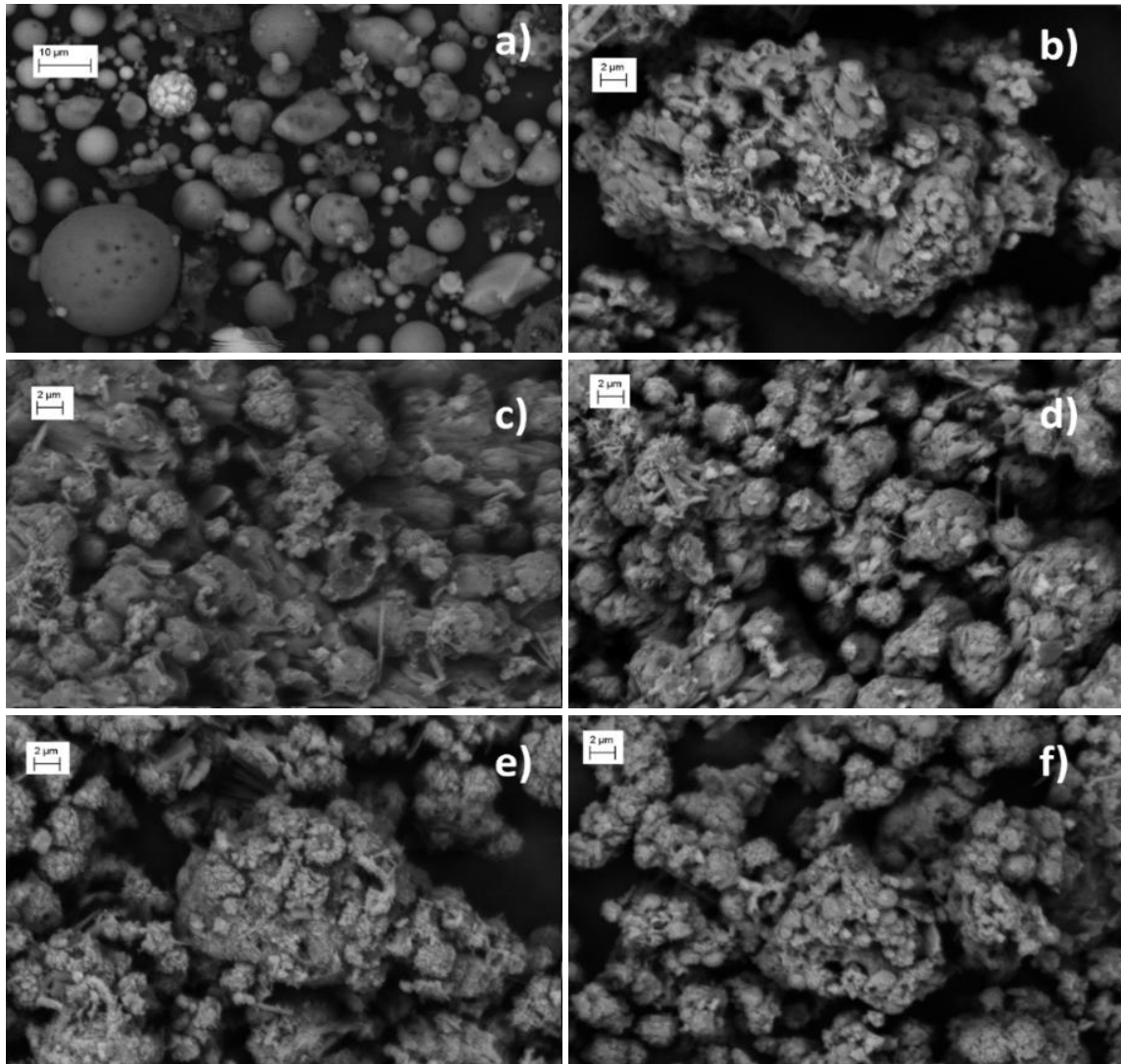


Figure 3. SEM images of a) CFA, b) M18, c) M7, d) M11, e) M14 and f) M15 samples.

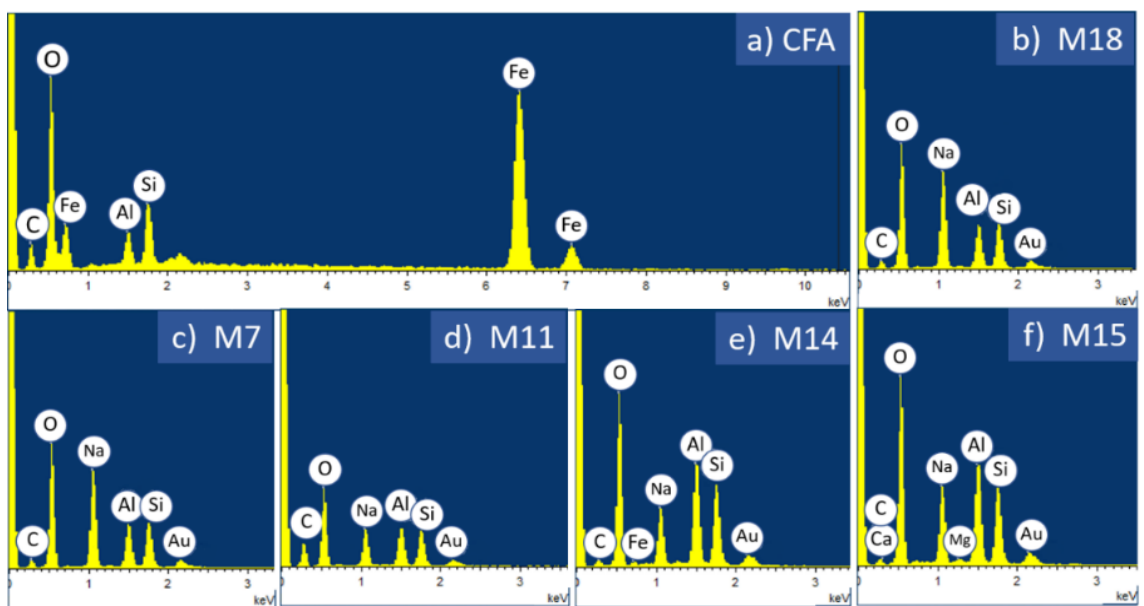


Figure 4. EDX analysis of a) CFA, b) M18, c) M7, d) M11, e) M14 and f) M15 samples. Au signal come from gold coating.

4. Conclusions

CFA selected from Sochagota TermoPaipa IV power station has chemical characteristics suitable to be used as zeolite precursor. For experimental conditions: activation time between 4.5 h and 43,5 h, temperature of synthesis between 60°C and 99.5°C and NaOH concentration between 2 M and 4.63 M, sodalite, Losod and P1-Na zeolites were obtained. The statistical analysis demonstrates that the temperature of synthesis is the main factor that affects the synthesis joined with the interaction between temperature and concentration of alkaline activator.

Acknowledgements

This work was financed by the Gobernación de Boyacá Grant N° 733 Colciencias and supported by Universidad Antonio Nariño Project N° 2017215.

References

- [1] Q. Xavier, P. Felicià, A. Andrés, and L-S. Angel, "Synthesis of Na-zeolites from fly ash," *Fuel*, vol. 76, pp. 793-799, 1997.
- [2] Y. Hefni, Y. A. El Zaher, and M. Abdel Wahab, "Influence of activation of fly ash on the mechanical properties of concrete," *Construction and Building Materials*, vol. 172, pp. 728-734, 2018.
- [3] R. Mistry and T. Kumar Roy, "Effect of using fly ash as alternative filler in hot mix asphalt," *Perspectives in Science*, vol. 8, pp. 307-309, 2016.
- [4] F. Fan, Z. Liu, G. Xu, H. Peng, and C. Cai, "Mechanical and thermal properties of fly ash based geopolymers," *Construction and Building Materials*, vol. 160, pp. 66-81, 2018.
- [5] J. Yu, Y. Yang, W. Chen, D. Xu, H. Guo, K. Li, and H. Liu, "The synthesis and application of zeolitic material from fly ash by one-pot method at low temperature," *Green Energy & Environment*, vol. 1, pp. 166-171, 2016.
- [6] S. C. Colin, and A. C. Paul, "The hydrothermal synthesis of zeolites: Precursors, intermediates and reaction mechanism," *Microporous and Mesoporous Materials*, vol. 82, pp. 1-78, 2005.
- [7] E. B. G. Johnson, and E. A. Sazmal, "Hydrothermally synthesized zeolites based on kaolinite: A review," *Applied Clay Science*, vol. 97, pp. 215-221, 2014.
- [8] R. M. Ramírez-Zamora, M. Solís-López, I. Robles-Gutierrez, Y. Reyes-Vidal, and F. Espejel-Ayala, "A Statistical Industrial Approach for the Synthesis Conditions of Zeolites Using Fly Ash and Kaolinite," *Environmental Progress & Sustainable Energy*, vol. 37, pp. 318-332, 2018.
- [9] A. Moutsatsou, E. Stamatakis, K. Hatzitzotzia and V. Protonotarios, "The utilization of Ca-rich and Ca-Si-rich fly ashes in zeolites production," *Fuel*, vol. 85, pp. 657-663, 2006.
- [10] R. Peña Penilla, A. Guerrero Bustos, and S. Goñii Elizalde, "Immobilization of Cs, Cd, Pb and Cr by synthetic zeolites from Spanish low-calcium coal fly ash," *Fuel*, vol. 85 pp. 823-832, 2006.
- [11] A. Derkowski, W. Franus, E. Beran and Adriana Czimerová, "Properties and potential applications of zeolitic materials produced from fly ash using simple method of synthesis," *Powder Technology*, vol. 166, pp. 47-54, 2006.
- [12] O. B. Kotova, I. N. Shabalin, D. A. Shushkov, and L. S. Kocheva, "Structural, Functional and Bioceramics. Hydrothermal synthesis of zeolites from coal fly ash," *Advances in Applied Ceramics*, vol. 115, pp. 152-157, 2016.
- [13] M. Wdowin, M. M. Wiatros-Motyka, R. Panek, A. L. Stevens, W. Franus and C. E. Snape, "Experimental study of mercury removal from exhaust gases," *Fuel*, vol. 128, pp. 451-457, 2014.
- [14] Z. Adamczyk, and B. Bialecka, "Hydrothermal Synthesis of Zeolites from Polish Coal Fly Ash," *Polish Journal of Environmental Studies*, vol. 14, pp. 713-719, 2005.
- [15] A. M. Cardoso, A. Paprocki, L. S. Ferret, C. M. N. Azevedo, and M. Pires, "Synthesis of zeolite Na-PI under mild conditions using Brazilian coal fly ash and its application in wastewater treatment," *Fuel*, vol. 139, pp. 59-67, 2015.
- [16] N. Shigemoto, H. Hayashi, and K. Miyaura, "Selective formation of Na-X zeolite from coal fly ash by fusion with sodium hydroxide prior to hydrothermal reaction," *Journal of Materials Science*, vol. 28, pp.4781-4786, 1993.
- [17] V. K. Jha, M. Nagae, M. Matsuda, and M. Miyake, "Zeolite formation from coal fly ash and heavy metal ion removal characteristics of thus-obtained Zeolite X in multi-metal systems," *Journal of Environmental Management*, vol. 90, pp. 2507-2514, 2009.
- [18] X. Ren, L. Xiao, R. Qu, S. Liu, D. Ye, H. Song, W. Wu, C. Zheng, X. Wu, and X. Gao, "Synthesis and characterization of a single phase zeolite A using coal fly ash," *RSC Advances*, vol 8, pp. 42200-42209, 2018.
- [19] K. Ojha, N. C. Pradhan, and A. N. Samanta, "Zeolite from fly ash: synthesis and characterization," *Bulletin of Materials Science*, vol. 27, pp. 555-564, 2004.
- [20] K. He, Y. Chen, Z. Tang, and Y. Hu, "Removal of heavy metal ions from aqueous solution by zeolite synthesized from fly ash," *Environmental Science and Pollution Research*, vol. 23, pp. 2778-2788, 2016.
- [21] N. M. Musyoka, L. F. Petrik, E. Hums, A. Kuhnt, and W. Schwieger, "Thermal stability studies of zeolites A and X synthesized from South African coal fly ash," *Research on Chemical Intermediates*, vol. 41, pp. 575-582, 2015.
- [22] R. R. Padhy, R. Shaw, S. Tiwari, and S. K. Tiwari, "Ultrafine nanocrystalline mesoporous NaY zeolites from fly ash and their suitability for eco-friendly corrosion protection," *Journal of Porous Materials*, vol. 22, pp. 1483-1494, 2015.
- [23] A. E. Ameh, O. O. Fatoba, N. M. Musyoka, and L. F. Petrik, "Influence of aluminium source on the crystal structure and framework coordination of Al and Si in fly ash-based zeolite NaA," *Powder Technology*, vol. 306, pp. 17-25, 2017.
- [24] M. Inada, H. Tsujimoto, Y. Eguchi, N. Enomoto, and J. Hojo, "Microwave-assisted zeolite synthesis from coal fly ash in hydrothermal process," *Fuel*, vol. 84, pp. 1482-1486, 2005.

- [25] T. Fukasawa, A. D. Karisma, D. Shibata, A. N. Huang, and K. Fukui, "Synthesis of zeolite from coal fly ash by microwave hydrothermal treatment with pulverization process," *Advanced Powder Technology*, vol. 28, pp. 798-804, 2017.
- [26] A. B. Marcos, E. S. Ricardo, P. O. Eliane, S. V. Leonardo, and A. E. Luciane, "Response surface methodology (RSM) as a tool for optimization in analytical chemistry," *Talanta*, vol. 76, pp. 965-977, 2008.
- [27] L. Zhou, Y.L. Chen, X. H. Zhang, F. M. Tian, and Z. N. Zu, "Zeolites developed from mixed alkali modified coal fly ash for adsorption of volatile organic compounds," *Materials Letters*, vol. 119, pp.140-142, 2014.
- [28] K. Byrappa, and M. Yoshimura, *Handbook of Hydrothermal Technology*. New Jerse, Noyes Publications, 2001.